

of the beam was determined with each of the two beam stages from the excitation curves for the dipole magnets. After about 15% of the experiment was completed it was discovered that two quadrupoles were misaligned. These quadrupoles were adjusted. This changed the calculated beam momentum for the corresponding stage by 0.5%. This correction was made to the early 15% of the data. At 4 BeV/c, the two stages disagreed in their prediction of the absolute beam momentum by less than 0.1%. A 0.1% change in the beam momentum corresponds to a shift in the A_2 mass scale of approximately 0.8 MeV.

⁹The proton-momentum resolution had a σ better than 1.1% for all momenta. (For calculating the A_2 mass resolution, $\sigma=1.1\%$ was used for the momentum resolution of the recoil proton.) The time resolution had $\sigma=0.4$ nsec. The proton path length was ~ 3.5 m. Thus, it was trivial to eliminate the 5–10% of events caused by triggers due to π 's, K 's, or d 's in the proton arm.

¹⁰In the determination of the absolute beam momentum, the two beam stages disagreed by 1.2% at 1 BeV/c. (The excitation curves are not accurately measured for all the magnets at this low momentum.) This corresponds to an uncertainty of the location of the π peak of 0.007 BeV².

¹¹The spatial resolution for the proportional chambers, which had 2-mm wire spacings, had $\sigma=0.8$ mm. For the spark chambers, which had 1-mm wire spacings, σ was 0.6 mm.

¹²Figure 3 shows results that are weighted to correct for the geometric acceptance. The average weight from 1.275 to 1.355 BeV is 1. The weight varies gradually in this region, changing by about 12% and 32% for the data in Figs. 3(a) and 3(b), respectively.

¹³For each event the standard deviation of the resolution function is calculated. The calculation uses the information given above in Refs. 8, 9, and 11, and determines the proton multiple Coulomb scattering by the Rosenfeld formula from Ref. 6. The scattering in the aluminum wires in the first proton spark chamber is treated statistically. We include the effects of the off-diagonal terms in the error matrix. The σ 's for the individual events have a distribution with a full width at half-maximum of 2.4 MeV and an average value of 3.9 MeV.

¹⁴The formulas that we used are given in Ref. 5. The width of the Breit-Wigner resonance was fixed at 95 MeV in these fits. A dipole width of 28 MeV was used.

¹⁵The distribution most suggestive of a dipole shape is an A_2^- plot with $-0.45 \leq t \leq -0.25$ (BeV/c)² and a vertex cut which reduces the experimental resolution—for this t range—from 3.5 to 3.4 MeV. The data discarded by the vertex cut have a resolution of 3.8 MeV. At the A_2^- peak there are 750 events per 5 MeV. These data were fitted by the Breit-Wigner and dipole formulas. The χ^2 values for 43 degrees of freedom were 59.2 and 90.9, respectively. The results were sensitive to the binning.

Resonant Spin Rotation—a New Lepton $g-2$ Technique*

G. W. Ford, James L. Luxon, and Arthur Rich†

The Harrison M. Randall Laboratory of Physics, The University of Michigan, Ann Arbor, Michigan 48104

and

John C. Wesley

*The Harrison M. Randall Laboratory of Physics, The University of Michigan, Ann Arbor, Michigan 48104,
and Gibbs Laboratory, ‡ Yale University, New Haven, Connecticut 06520*

and

V. L. Telegdi‡

*Enrico Fermi Institute and Department of Physics, The University of Chicago, Chicago, Illinois 60637, and
CERN, Geneva, Switzerland*

(Received 5 June 1972)

We describe an extension of the Michigan g -factor work that permits measurement of the $g-2$ precession frequency of free leptons by a resonance technique. Preliminary results with electrons (accurate to about 100 ppm in the anomaly) indicate that the technique may be of use in various future experiments.

Recent precision measurements of lepton g -factor anomalies can be classified as being either "precession experiments" or "resonance experiments," depending on the technique em-

ployed.¹ Precession experiments include measurements of the electron,² positron,³ and muon⁴ anomalies. The characteristic feature of these experiments is a direct observation of the spin

motion of polarized leptons in a static magnetic field. The resonance technique has to date been limited to electron anomaly measurements.^{5,6} The characteristic feature of these experiments is the presence of an oscillating electromagnetic field used to induce transitions between the energy eigenstates of a lepton interacting with a static magnetic field. We describe here a variation of the most recent Michigan electron $g-2$ work² that permits measurement of the $g-2$ precession frequency by a resonance method. Preliminary tests indicate that the potential accuracy is similar to the precession method, and that certain characteristics of the new method may be useful in future experiments.

The method used to determine the $g-2$ frequency is based on a resonant perturbation of the spin motion observed in previous Michigan $g-2$ experiments. This motion can be summarized as follows: Consider an electron with velocity \vec{v} and polarization \vec{S} undergoing planar cyclotron motion in a uniform magnetic field $\vec{B}_0 = B_0 \hat{z}$. The relative precession of \vec{S} with respect to \vec{v} will occur at a difference or $g-2$ frequency ω_D given by $\omega_D = a\omega_0$, where $a = \frac{1}{2}(g-2)$ is the g -factor anomaly and $\omega_0 = eB_0/mc$. Because of the $g-2$ precession, the helicity $\hat{S} \cdot \hat{v}$ will vary as $\cos\omega_D T$, T being the time spent by the electrons in the magnetic field. If N oscillations of $\hat{S} \cdot \hat{v}$ are observed between $T = T_1$ and $T = T_2$, then $\omega_D = 2\pi N / (T_2 - T_1)$. We refer to this means of measuring ω_D as the "cycle counting" method.

The alternate means which we have used to determine ω_D is illustrated in Fig. 1. A current-carrying wire oriented parallel to \vec{B}_0 is placed at the center of the electron orbit generating an azimuthal field \vec{B}_θ . For an electron with \vec{S} initially perpendicular to both \vec{B}_0 and \vec{v} , the torque $\vec{\mu} \times \vec{B}_\theta$ on the electron magnetic moment $\vec{\mu}$ (antiparallel to \vec{S}) will tend to rotate \vec{S} out of the orbital plane. At the same time, the component of \vec{S} in the orbital plane precesses at frequency ω_D about \hat{z} . If, after half of a $g-2$ period, \vec{B}_θ has reversed direction, the resultant torque will continue to rotate \vec{S} out of the orbital plane. Thus, if the θ field oscillates at frequency $\omega = \omega_D$, the time-average torque experienced by the orbiting electron will rotate \vec{S} towards \vec{B}_0 .

The apparatus is identical to that described in Refs. 1 and 2 with the addition of a wire along the axis of the trapping cylinders and a frequency synthesizer to supply the rf current. Transversely polarized electrons prepared by Mott scattering are injected into a weak magnetic mirror

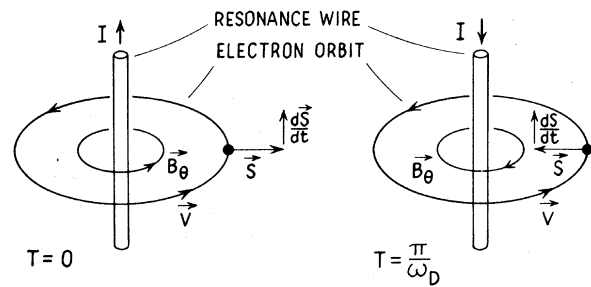


FIG. 1. Rotation of the spin \vec{S} by the θ field.

trap at $T = 0$. After being held in the trap for a predetermined length of time, the electrons are ejected from the trap to undergo a second Mott scattering which serves to measure their polarization. The counting rate exhibits an asymmetry

$$R(T) = R_0 [1 + \delta \cos(\omega_D T + \varphi)], \quad (1)$$

where R_0 is the counting rate for an unpolarized beam, φ is a phase angle, and δ is an asymmetry parameter proportional to the component of the electron polarization in the orbital plane at the time of the second scattering. During the entire time the electrons are trapped, a constant-amplitude rf current in the central wire generates a weak oscillating θ field $\vec{B}_\theta = 2B_1 \cos(\omega t) \hat{\theta}$ at the electron orbit. Because of the spin rotation caused by the θ field, both δ and φ are functions of the amplitude and frequency of the rf current. To determine ω_D , one measures δ as a function of ω , while holding all other experimental parameters (including B_1) constant. The minimum in $\delta(\omega)$ corresponds to ω_D .

The parameters δ and φ were measured by sampling $R(T)$ over a short interval near $T = 1700$ μsec . A least-squares fit to measurements of $R(T)$ versus T was used to determine δ and φ .² Asymmetry data were collected with the rf alternately switched on and off for 1-sec periods. The result of each data run was normalized by computing the ratio $A = \delta(\text{rf on}) / \delta(\text{rf off})$ and the phase shift $\Delta\varphi = \varphi(\text{rf on}) - \varphi(\text{rf off})$. This procedure eliminates the effect of any variations in δ and φ arising from drifts in the experimental parameters.

For a quantitative description, it is necessary to discuss the equation of motion for \vec{S} in the presence of the oscillatory field:

$$d\vec{S}/dt = [\omega_D \hat{z} + 2\omega_1 \hat{v} \cos(\omega t + \eta)] \times \vec{S}. \quad (2)$$

This equation is familiar from magnetic resonance, where in the near-resonant case it is solved⁷ by transforming to a frame R rotating

with angular velocity ω about \hat{z} , and dropping terms which oscillate at frequency 2ω . The resulting equation in R is

$$d\vec{S}_R/dt = [\delta\omega\hat{z} + \omega_1(\hat{v}\cos\eta + \hat{z}\times\hat{v}\sin\eta)]\times\vec{S}_R, \quad (2')$$

where $\delta\omega = \omega_D - \omega$. This equation is similar to (1); it describes a motion in which the polarization $\vec{S}_R(t)$ precesses with frequency $\omega_{er} = (\delta\omega^2 + \omega_1^2)^{1/2}$ about the direction

$$\hat{n} = \frac{\delta\omega}{\omega_{er}}\hat{z} + \frac{\omega_1}{\omega_{er}}(\hat{v}\cos\eta + \hat{z}\times\hat{v}\sin\eta). \quad (3)$$

$$\langle\vec{S}(t)\rangle = (2A-1)(\hat{z}\cdot\vec{S}_0)\hat{z} + A\{\cos[\omega_D t + \Delta\varphi(t)][\vec{S}_0 - (\hat{z}\cdot\vec{S}_0)\hat{z}] + \sin[\omega_D t + \Delta\varphi(t)][\hat{z}\times\vec{S}_0]\}, \quad (5)$$

where

$$A = 1 - (\omega_1/\omega_{er})^2 \sin^2(\omega_{er}t/2). \quad (6)$$

and

$$\Delta\varphi(t) = \delta\omega t + \tan^{-1} \frac{2\omega_{er}\delta\omega \sin\omega_{er}t}{\omega_1^2 + (2\delta\omega^2 + \omega_1^2)\cos\omega_{er}t}. \quad (7)$$

Note that $A(t)$ and $\Delta\varphi(t)$ are slowly varying compared with the fast spin precession (at rate $\approx\omega_D$) in the orbit plane. The phase-averaged polarization $\langle\vec{S}(t)\rangle$ described by Eq. (5) thus corresponds to a *resonant depolarization*.

The functions A and $\Delta\varphi$ are plotted in Fig. 2 in terms of the angles $\Phi_0 \equiv (\delta\omega)T$ and $\Theta_0 \equiv \omega_1 T$, which have an obvious geometrical significance in the rotating frame. The experimental mea-

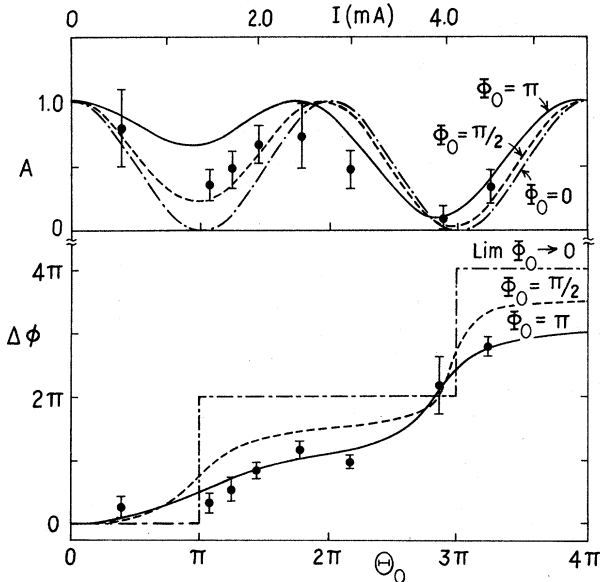


FIG. 2. Expected amplitude A and phase shift $\Delta\varphi$ of the asymmetry as a function of the resonant rotation Θ_0 . The data points obtained and the rf current used are superposed.

In the present experiment, the initial polarization \vec{S}_0 is fixed, but the phase of the oscillating current at $t=0$ is random. To obtain the $\vec{S}(t)$ corresponding to the experiment, one must hence perform an average over η . This is done using the results

$$\langle\hat{n}\rangle = (\delta\omega/\omega_{er})\hat{z},$$

$$\langle n_i n_j \rangle = \left(\frac{\delta\omega}{\omega_{er}}\right)^2 \hat{z}_i \hat{z}_j + \frac{1}{2} \left(\frac{\omega_1}{\omega_{er}}\right)^2 (\delta_{ij} - \hat{z}_i \hat{z}_j). \quad (4)$$

Transforming back to the velocity-fixed coordinate frame, we obtain

measurements at $\omega/2\pi = 3.431\,000$ MHz (the anticipated resonance frequency) are superimposed. The overall horizontal (current) scale of the data points has been adjusted with respect to the Θ_0 scale so as to yield the best possible joint fit to both the amplitude and phase curves. Fitting the current scale provides a determination of ω_1 that can be compared with the value calculated directly from the measured rf current and orbit radius. In Fig. 2, the first amplitude minimum (near $\Theta_0 + \pi$) occurs at $I \cong 1.4$ mA. Using $\Theta_0 = \pi$ and $N = 5800$, the fitted data imply that 1.4 mA corresponds to $\omega_1 = (1.9 \pm 0.4) \times 10^3$ sec $^{-1}$. A direct calculation using $\omega_1 \cong eI/\gamma ac^2 \rho_0$ gives $\omega_1(1.4 \text{ mA}) = 2.1 \times 10^3$ sec $^{-1}$. These data also imply a value for Φ_0 . The best fit to the amplitude data occurs for $\Phi_0 \cong \pi/2$, while the best fit to the phase-shift data occurs for $\Phi_0 \cong \pi$. On the basis of the data plotted in Fig. 2, we estimate that $\Phi_0 = 2.4 \pm 0.8$ rad.

A series of measurements of A was made at various frequencies with $I = 1.5$ mA. The results of these runs are shown in Fig. 3, with the two fitted curves superimposed. The solid curve (1) shows the expected resonance line for $\Theta_0 = 3.5$ and $\Phi_0 = 2.4$ at $\omega/2\pi = 3.431\,000$ MHz, as deter-

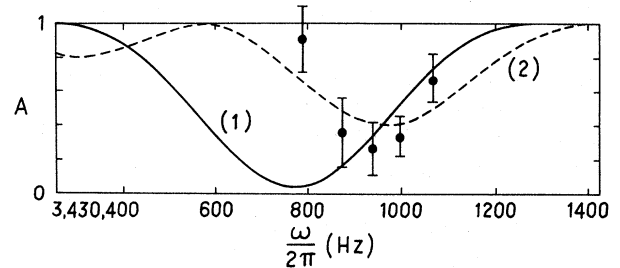


FIG. 3. Two possible fits of the line-shape data to the theoretical line shape.

mined from the measurements plotted in Fig. 2. There are no adjustable parameters. The fit would be satisfactory except for the lowest-frequency point. In the dashed curve (2) both the center frequency and Θ_0 were varied to obtain the best fit. The resultant fit is much better, but the value of $\Theta_0 = 4.5$ at a current of 1.5 mA does not agree with the data of Fig. 2. More important, the center of frequency of the resonance is approximately 3.431 000 MHz. This implies that amplitude and phase measurements made at this frequency should give $\Phi_0 \cong 0$, in obvious contradiction to the results shown in Fig. 2.

In the absence of stray electric fields in the trapping region, the difference frequency expected in the data runs is $3\,431\,000 \pm 70$ Hz, as calculated from measurements of the magnetic field and $a = (1\,159\,657 \pm 3.5) \times 10^{-9}$.² If electric fields are present, ω_D will be shifted by 4 ppm (13 Hz) per mV/cm of average radial electric field component.² The offset of curve (1) can be attributed to a radial field of 14 mV/cm, a field which is not inconsistent with those observed in $g - 2$ experiments with electrodes inside the orbit.⁸ An attempt to use the cycle-counting method to measure ω_D with the wire in place, but with no applied rf, failed to rule out the presence of a field consistent with the offset of curve (1). Unfortunately, a major breakdown of the apparatus terminated the experiment before further tests could be completed. The small number and limited frequency range of the data points in Fig. 3 make unambiguous determination of the center of the resonance impossible. However, the various problems associated with interpreting the data are concerned with effects which are less than the intrinsic width of the resonance line. Our present results do verify all essential features of the effect.

The resonance method offers several promising possibilities for future work. Insofar as statistical accuracy is concerned, the precision of an optimized resonance experiment at best equals that of a cycle-counting experiment. However, using the resonance wire to rotate \vec{S} parallel to \vec{B}_0 (possible if the rf is phase locked to the injection pulse) may permit an improved positron $g - 2$ experiment. In previous positron experiments, polarization analysis was based on positronium formation in a plastic scintillator immersed in a magnetic field \vec{B}_p . The asymmetry observed was proportional to $\vec{S} \cdot \vec{B}_p$. Since the optimum value of B_p is about 10 kG, a field separate from the much weaker trapping field was

necessary, and this caused a number of experimental difficulties. However, by trapping the positrons in a field $B_0 = 10$ kG (under consideration for future work¹), using the resonance wire to rotate \vec{S} parallel to \vec{B}_0 , and then forming positronium in the same field, one can determine ω_D by measuring $\vec{S} \cdot \vec{B}_0$ as a function of ω . Such a positron $g - 2$ experiment should yield an order of magnitude increase in precision over the last effort.

It might also be interesting to try to extend this scheme to electrons (or even muons), since it is simpler from a timing and data collection standpoint to observe the slow rotation of \vec{S} into \vec{B}_0 , than it is to observe the $g - 2$ precession curve. Unfortunately we know of no scheme for measuring $\vec{S} \cdot \vec{B}_0$ for electrons in a manner compatible with other $g - 2$ requirements.

Finally, it may be possible to apply this technique to a measurement of the magnetic moment of the proton in nuclear magnetons μ_p/μ_N . Since $\mu_p/\mu_N = \omega_s/\omega_c$ and $\omega_D = \omega_s - \omega_c$, μ_p/μ_N could be measured by applying the present technique for measuring ω_D to polarized protons in a magnetic well along with our recently developed method for measuring ω_c (rf resonance on unpolarized protons in a magnetic well).⁹ We would then be comparing two resonance lines from identical samples of free protons instead of deriving ω_s from NMR measurements on water samples, as is the current practice.

Theoretical calculations for this work were carried out by G.F. and V.T. while J.L., A.R., and J.W. carried out the experimental investigation. The authors have greatly benefitted from discussions with many colleagues, particularly Professor R. Winston of Chicago.

*Experimental work at the University of Michigan supported through a National Bureau of Standards Precision Measurements Grant No. 1-35897 to A.R.

†On leave, winter 1973, at Observatoire de Paris, Section d'Astrophysique, Meudon, France.

‡Present address. Work supported in part by the U. S. Atomic Energy Commission under Contract No. AT (11-1)-3075.

§Work supported by the National Science Foundation under Contract No. GP29575A#1.

¹A. Rich and J. Wesley, *Rev. Mod. Phys.* **44**, 250 (1972).

²J. Wesley and A. Rich, *Phys. Rev. A* **4**, 1341 (1971).

³J. Gilleland and A. Rich, *Phys. Rev. A* **5**, 38 (1972).

⁴J. Bailey, W. Bartl, G. von Bochmann, R. C. A. Brown, F. J. M. Farley, M. Giesch, H. Jostlein, S. van

der Meer, E. Picasso, and R. W. Williams, to be published.

⁵G. Gräff, E. Klempt, and G. Werth, *Z. Phys.* **222**, 201 (1969).

⁶F. Walls, Ph. D. thesis, University of Washington, 1970 (unpublished).

⁷See, e.g., N. F. Ramsey, *Molecular Beams* (Oxford

Univ. Press, Oxford, England, 1956), p. 146 et seq. The present notations are kept close to Ramsey's to make analogies evident.

⁸D. T. Wilkinson and H. R. Crane, *Phys. Rev.* **130**, 852 (1963).

⁹J. L. Luxon and A. Rich, *Phys. Rev. Lett.* **29**, 665 (1972).

Possible Existence of a New Y^* Resonance at 1930 MeV

S. Dado, A. Birman, J. Goldberg, and H. Weiss

Department of Physics, Technion—Israel Institute of Technology, Haifa, Israel

(Received 27 September 1972)

A new resonant wave with unknown isospin and $J^P = \frac{7}{2}^-$ ($\frac{9}{2}^-$ not completely excluded) is found to be necessary in order to explain the energy dependence of the higher Legendre polynomial coefficients (A_6 , A_7 , and A_8) in the expansion of the K^-p elastic scattering differential cross section between 1937 and 1991 MeV. Assignment of this tentative resonance to a $\frac{7}{2}^-$ octet with the known $N(2190)$ and $\Lambda(2100)$ is found to be reasonably good.

A Legendre polynomial expansion of the differential cross section $d\sigma_{el}/d\Omega$ of K^-p elastic scattering at five energies approximately equally spaced between 1937 and 1991 MeV requires coefficients up to order 8 at the second energy (1950 MeV). Around this energy the higher expansion coefficients (A_6 , A_7 , and A_8) display a peculiar structure.

The data are obtained from 100 000 photographs of the Saclay-CERN 81-cm hydrogen bubble chamber placed in a K^- beam from the CERN proton synchrotron, tuned to nominal momenta of 1.31, 1.34, 1.37, 1.40, and 1.43 GeV/c. Out of about 22 000 two-prong events, 8258 were essentially nonambiguous elastic scattering events. The differential cross sections were corrected for loss of short (low energy) protons and for azimuthal anisotropy¹ and normalized by interpolation of total tabulated cross sections.² This was done after checking the consistency of our total cross

sections obtained from the scanning of all types of events and the counting of three-charged-body decays in the beam.³ The differential cross section $d\sigma_{el}/d\Omega$ was expanded in a series of Legendre polynomials:

$$d\sigma_{el}/d\Omega = \lambda^2 \sum_{l=0}^{l_{\max}} A_l P_l(\cos\theta^*), \quad (1)$$

where θ^* is the angle between the incoming and outgoing mesons in the center-of-mass system and λ is the reduced center-of-mass wavelength.

In addition to the elastic cross section, Table I displays the χ^2 obtained for the least-squares fit, depending upon l_{\max} . From this table it is clear that $l_{\max} = 8$ is necessary to obtain a stable χ^2 . This is a convenient way to summarize several arguments³ showing that this effect is not due to biases and/or to statistical fluctuations.

Figure 1 shows the variation of A_6 , A_7 , and

TABLE I. Elastic cross sections and χ^2 as a function of the order of the fit (l_{\max}). N is the number of degrees of freedom.

| Energy (MeV) | σ_{el} (mb) | χ^2 | | | | | | |
|-----------------|-----------------------|------------------------|------------------------|------------------------|------------------------|------------------------|------------------------|-------------------------|
| | | $l_{\max}=4$ $N=34$ | $l_{\max}=5$ $N=33$ | $l_{\max}=6$ $N=32$ | $l_{\max}=7$ $N=31$ | $l_{\max}=8$ $N=30$ | $l_{\max}=9$ $N=29$ | $l_{\max}=10$ $N=28$ |
| 1937 | 10.93 ± 0.33 | 66.29 | 45.69 | 43.56 | 41.58 | 41.48 | 40.83 | 40.77 |
| 1950 | 10.32 ± 0.31 | 84.36 | 48.01 | 46.10 | 37.79 | 26.10 | 25.48 | 25.26 |
| 1964 | 9.48 ± 0.28 | 82.40 | 48.11 | 47.32 | 42.85 | 42.13 | 42.12 | 37.75 |
| 1977 | 9.26 ± 0.28 | 98.07 | 39.80 | 39.80 | 28.94 | 28.66 | 27.81 | 25.37 |
| 1991 | 8.69 ± 0.26 | 94.75 | 39.36 | 38.75 | 19.08 | 18.61 | 17.73 | 17.72 |